Boosting Network Resiliency with Microgrid-based Distribution Networks Planning

Hassan Jahangirzadeh[1], Sajad Najafi Ravadanegh[1,*], and Navid Taghizadegan Kalantari[2]

[1] *Resilient Smart Grids Research Lab, Azarbaijan Shahid Madani University, Tabriz, Iran*
[2] *Department of Electrical Engineering, Azarbaijan Shahid Madani University, Tabriz, Iran*
**Corresponding author: s.najafi@azaruniv.ac.ir*

Manuscript received 21 January, 2025; revised 24 February, 2025; accepted 16 August, 2025. Paper no. JEMT-2501-1539.

In this paper, resilient microgrid is designed and compared with an optimal conventional network at the same area subjected to a weather-related hurricane. Comparisons are made with both network total cost and its resiliency indicators. For MGs-based network the geographical boundaries of each MG is supposed to be predefined while their electrical network boundaries are designed as an integrated distribution network. The costs of different parts of the network such as low and medium voltage feeders, distributed energy resources (DERs), and substations are compared with the resilient-based network. The resiliency of the designed distribution network against the hurricane is explored using components fragility index. To evaluate the components fragility index, the study area is divided into several GIS-based zones in terms of wind intensity. The resilience of the planned network is evaluated in three modes as normal, reinforced distribution network and in the presence of MGs. A sensitivity analysis is also performed at different wind speeds scenarios. To evaluate the effectiveness and comparison of the network performance several resilience indexes are used. Based on the results, the energy not supply for the normal case is 22416.36 kwh while it is reduced to 7377.54 kwh in case of network hardening. The ENS decrease to 20831.67 kwh in case on MG-based network planning. Results indicate that at higher wind speed the performance of MG-based network is better comparing to reinforced conventional network.

Keywords: *Distribution network; Planning, Resiliency; Hurricane; Fragility curve; Geographical information system.*

http://dx.doi.org/10.22109/jemt.2025.501372.1539

Nomenclature

Indexes

ALDF	The annual average of load factor in the substation
ALSF	The annual average of loss factor in the substation
$Cons_{FC}^{HSub}$	Construction cost of Sub-distribution substation, $
$Cons_{FC}^{MF}$	Construction cost of MV feeders, $
$Cons_{FC}^{MSub}$	Construction cost of distribution substation, $
$Cost_{VOM}$	O&M variable cost, $/MWh
$Cost_{FOM}$	fixed O&M cost, $/MWh
$Cost_{LE}$	Levelized cost of energy, $/kWh
DG_i	i-th candidate DG
DG_{FC}	Financing cost of DG in $
$HSub_{FC}$	Financing cost of Sub-distribution substation, $
L_i	Length of i-th MV feeder, m
$Loss_{FC}^{HSub}$	Loss cost of Sub-distribution substation, $
$Loss_{FC}^{MF}$	Loss cost of MV feeders, $
$Loss_{FC}^{MSub}$	Loss cost of distribution substation, $
MF_{FC}	Financing cost of MV feeders, $
$MSub_{FC}$	Financing cost of distribution substation, $
MF_i	i-th MV feeder
$MSub_i$	i-th distribution substation
$N_{LDER,i}$	Number of DG downstream of i-th MV or HV substation
$N_{LMSub,i}$	Number of substations below i-th distribution substations
NMSub	The number of candidate distribution substation
N_{SMF}	Number of selected MV feeders
$N_{UMF,i}$	Number of feeders in upstream of i-th substation
Out_{FC}^{HSub}	Power outage cost for sub-distribution substation, $
Out_{FC}^{MF}	Subscriber's power outage cost of MV feeders, $
Out_{FC}^{MSub}	Subscriber's power outage cost of distribution substation, $
R_0	The amount of resiliency (power) before the event

R_{pd}	The amount of resiliency (power) after the event
S_{MSub}	Set of all candidate medium voltage substations
SPL	Load, kVA for MV/HV substation and kW for DG
S_{SMF}	Set of selected MV feeders
$Total_{FC}$	Total financing cost, $
t_{pre}	Pre- event time
t_{poe}	Post- event time
t_{prr}	Pre- restoration time
t_{por}	Post- restoration time
x_i	X-coordinate of i-th knot, m
$x(m)$	Longitude of the study area, meter
y_i	Y- coordinate of i-th knot, m
$y(m)$	Latitude of the study area, meter
κ_i	Decision variable (Binary) for i-th DER
λ_i	Decision variable (Binary) for i-th MVS

Variables

CC	Construction cost, $/km for feeders, $/ KVA for substations and $/kW for distributed generations
CCR	Construction cost, for MV lines after reinforcement
DD	Damage Duration, h/failure
DR	Damage rate
D_{Rate}	Discount rate
$Fuel_{Price}$	Price of fuel, $
$Heat_{Rate}$	Rate of heat
I	Line current, A
I_{max}	Line nominal current, A
LT_{MSub}	Lifetime of distribution substation, year
LT_{DER}	Lifetime of DG, year
N_{Blocks}	Total load blocks
OCR	Subscriber's power outage cost rate, $/KW
P	DG size, KW
P_j	The Power amount of j-th distribution substation, KW
P_k	The Power amount of k-th load point, KW
P_{NLL}	MV/HV substation no-load loss, kW
P_{SCL}	MV/HV substation short-circuit loss, kW
$P(w_i)$	Fragility probability for MV lines in i-th wind speed
R_i	Resistance of i-th MV line, Ω/m
R_{ij}	Resistance of line from node i to node j , Ω/m
S	MVS/HVS substation capacity, kVA
S_{max}	Maximum capacity of a MV/HV substation, kVA
T	Study horizons, year
TL	Current of MV/HV substation at operation period, p.u
Total CR	Total cost, for MV feeders after Reinforcement
TR_{Paid}	Tax rate paid
VD	Voltage drop, %
$VD_{MV,max}$	Maximum voltage drop in MV, %
V_{MV}	Medium voltage level voltage
w	wind speed (m/s)
$w_{critical}$	Wind speed with zero failure probability
$w_{collapse}$	Wind speed with failure probability equal to one
X_{ik}	Line reactance from node i to node j, Ω /m
X_j	Reactance of j-th MV feeder, Ω /m

Coefficients

CPF	Capacity factor
CRC	Capital recovery coefficient
PF	Power factor
PF_j	Power factor of j-th MV line
PF_k	Power factor of k-th load
RVP	Reducing the value of the present
RAF	Rated power factor to average delivery power
ρ	Coefficient of energy losses cost, $/kwh

Abbreviations

CHP	Combined Heat and Power
DG	Distributed generation
FC	Fuel cell
HSub	Sub-distribution substation
HV	High voltage
ICA	Imperialist Competitive Algorithm
MG	Microgrid
MV	Medium voltage
PV	Photovoltaic
WT	Wind Turbine

1. Introduction

Recently, the impact of weather and climate related hazards on power systems are increase dramatically. These hazards are usually classified as incidents with low probabilities and high impact, as their occurrence period may be low, but their impact may be very severe. The resiliency concept is reported for different sciences such as environmental systems [1], social systems [2], society [3], economics [4] and health networks [5]. Despite the slight difference between above definitions, the resiliency concept in each field (including electric power networks) can generally be defined as the ability of a system to anticipate and resist external incidents and return to pre-shock mode at the highest speed possible and better adaptation to future catastrophic accidents and preparedness against [6]. Defining and understanding the resilience of power systems against such catastrophic events is considered by many researcher [6]. A number of resilient studies that have been developed in previous years [7] include modeling methods and strategies for increasing resilience. In addition to the traditional reliability indices such as expected loss of energy [8], various indicators for determining the system's resilience are presented in particular. For example, in [9], resiliency is defined as the area ratio among the objective and actual functional curves. In [10], the resiliency of the system has been improved from corrupted mode by using the delivery function ratio. In [11] a proactive resource management model is presented for network infrastructure components repair and restoration damages to distribution network encountering with hurricane. An efficient framework is developed to minimize possible damages to network components with minimum cost. A MI equivalence is adapted for original model and consequently the problem is solved by the Benders' decomposition algorithm. Both transmission and distribution sector are considered in this paper. The

effects of new technology such as distributed generations and MGs is not considered in this paper. An optimal feeder hardening considering multiple temporary MGs method is proposed in [12] to improve network resiliency with robust optimization. A three-level optimization model is used to minimize the costs of line hardening and the operation of MGs and load shedding. At the first level, line hardening with discovering for the impact of the worst contingencies is solved. At the second level the max-min sub-problem is solved using linearization techniques. In this paper the application of robust optimization leads to a worst case solution that may increase network hardening cost as conservative method. In [13] a framework to enhance distribution networks resiliency against hurricane as a weather hazards is proposed including three resilience-oriented design indexes. These indexes involve network feeders hardening, backup DGs installing, and automatic switches placement. A Spatio-temporal correlation among resilient indexes decisions and uncertainties with capturing the failure-recovery cost and solving a large-scale mixed-integer stochastic problem is the main contribution of [13]. The minimizing of ROD investment cost in the first stage and the expected costs of loss of load, DG operation, and damage repairs in the second stage is solved in this paper. Similar to [11] in this paper the MG is not modeled for resiliency enhancement. In [14], a new resiliency evaluation framework is defined with respect to the concept of the triangle of resiliency, which states that all critical infrastructure stages, such as the power system that may remain in different modes during the hazards, as well as the transition between these transient states. Similar resonance curves have been presented in [9], but not fully and routinely modeled and determined. Indicators of time-dependent infrastructure and time-dependent utilization are based on different indices in [15] to determine the resilience. For example, how much does resiliency reduced and how fast it is, how long it takes to survive the failure after the event, and how long it takes for the system to be restored to the pre-event state. The actual modeling of the time-dependent time of an infrastructure exposed to severe events and the application of the distinction between the underlying effects and exploitation and then the construction and integration of these four criteria leads to an area, where using that area, you can observe the whole system's resilience in a total of all stages. The overall assessment framework is based on the weather conditions and the use of potentially fragile curves for the power system equipment. Several case studies have been presented on the British Transmission Experimental Network [16] to determine the infrastructure resilience and impact of incremental strategies using the framework of resiliency indicators. Generally, in the assessment of power system resilience, the following three-step procedure is used to indicate all stages during an accident, after an accident, and during recovery [17].

This paper includes some new aspects in optimal network planning with resiliency indexes. The application of GIS data can be one of the merits of the paper that facilitates the paper for practical application. Based-on the above discussion on some major published papers, some papers focus on the resilient planning of conventional distribution network, while the other considered the MGs as provisioning element for optimal resilient planning. One of the main question is that the resilient planning cost of distribution network how much increase with respect to conventional planning. In this paper a cost and resilient based planning for the MG-based distribution networks is evaluated and compared. For each MG all necessary requirements are considered with optimal cost and the feeder's route are optimized. Given that resilient network design leads to increased network costs, in this paper we divided the network into several zones in terms of wind intensity and designed the part of the network that is exposed to severe storms to be resilient to optimize the network design in terms of cost and resilience. The research gap addressed in this paper and not mentioned in other papers is how much the network costs increase if we want to increase the network resilience by a certain amount. This method leads to better decisions for network designers to choose the level of network resilience according to the budgets allocated for network design.

This paper focuses on integrated planning of a distribution network both in cases of hardening and MG-based design. In this regard we have two major contribution in this paper.

1- Integrated planning of distribution network with all MV, LV components is one of the novelty of this paper. Most of the papers are focused on just MV or LV network separately with the objective function of cost or reliability. While resiliency of the integrated network is major goal of this paper.

2- The future distribution network can be clusters of MG. Majority of current published papers studies the conventional distribution networks, while the second objective of this paper is planning of the integrated distribution network based on MGs considering network resiliency.

2. Problem formulation

In this section the mathematical modeling for different part of the networks such as MV and LV network, load and MGs are discussed. The candidate locations for medium voltage (MV) feeders, distributed energy resources (DERs), medium voltage (MV) and high voltage (HV) substation are given. The study area is divided into many square load blocks based-on the spatial load forecasting methods. In the design of the grid, three different phases are considered.

1- Determining the geographic boundaries of the MGs: In practice, in the electrical design of grid-based grid distribution networks, geographic boundaries may have been identified from the beginning. In this paper, MGs are based on geographic boundaries.

2- Design of distributed generation resources: Determining the location and optimal capacity of DERs in MGs with consideration of all network constraints is an important task. Each grid must also have at least one dispatchable energy resource to be able to supply part of its critical loads during a components failure due to hazard.

3- Determine the electric boundaries of the MGs: With the optimal switch placement in the distribution network, it is possible to separate the grid into interconnected MGs under different operating scenarios. In fact, the switches between MGs represent the electrical boundaries of the MGs, so that each MG, like a single power grid, can meet its internal demand.

2.1. Objective function

In both case of cost-based and resilient based planning the objective function consists of HV and MV substation, MV feeders and distributed generation sources costs according to (1) that in case of resilient-based planning the reinforcement of the network component and hardening leads to an extra cost [18]. Each of the four first section includes construction costs, losses cost, and their corresponding outages cost.

$$Total_{FC} = LF_{CF} + MSub_{CF} + DG_{CF} + MF_{CF} + HSub_{CF} \quad (1)$$

2.2. Modeling of distribution substation

The cost of a distribution substation includes the cost of construction, the cost of losses, and the cost of subscriber's power outage according to (2):

$$MSub_{CF} = Cons_{CF}^{MSub} + Loss_{CF}^{MSub} + Out_{CF}^{MSub} \cdot \quad (2)$$

The construction cost is calculated by Equation (3):

$$Cons_{CF}^{MSub} = \sum_{i=1}^{NMSub} CC(MSub_i) \cdot S(MSub_i) \cdot \frac{T}{LT_{MSub}} \cdot \lambda_i \cdot \quad (3)$$

The variable S represents the size of the distribution substation, which is calculated by sum of the connection loads to each post derived from equation (4).

$$SPL(MSub_i) = \frac{\sum_{k=1}^{NLP_i} P_k}{ALDF(MSub_i) \cdot PF(MSub_i)} \cdot \quad (4)$$

The cost of loss of distribution points is calculated as the (5):

$$Loss_{FC}^{MSub} = \sum_{i=1}^{NMSub} [P_{NLL}(MSub_i) + P_{SCL}(MSub_i) \cdot TL^2(MSub_i) \cdot ALSF(MSub_i)] \cdot \rho \cdot T \cdot 8760 \cdot \lambda_i \cdot \quad (5)$$

ALSF represents the average annual loss factor, which is calculated by equation (6) [19]. TL represents the load of MV substations at the time of operation (in p.u.), which is calculated from equation (7):

$$ALSF(MSub_i) = 0.15 \cdot ALDF(MSub_i) + 0.85 \cdot ALDF^2(MSub_i) \cdot \quad (6)$$

$$TL(MSub_i) = \frac{\sum_{k=1}^{NLP_i} P_k}{S(MSub_i) \cdot PF(MSub_i)} \cdot \quad (7)$$

The power outage cost for the MV substation is calculated from the (8):

$$Out_{CF}^{MSub} = \sum_{i=1}^{NMSub} \left[DD(MSub_i) + DR(MSub_i) \cdot \sum_{k=1}^{NLP_i} P_k \right] \cdot OCR \cdot T \cdot 8760 \cdot \lambda_i \cdot \quad (8)$$

2.3. Distributed energy resources modeling

It is assumed that the location and capacity of the DERs are already known as candidates. It is possible to calculate the cost of DERS from the (9) and using cost of energy leveled ($Cost_{EL}$), which is given in (10) [20-21]. The cost of energy leveled includes all fuel costs, maintenance, operation, and construction, and the energy price in dollars per kilowatt-hour.

$$DG_{CF} = \sum_{i=1}^{NMSub} \left[Cost_{EL}(DG_i) \cdot \frac{P(DG_i)}{RAF(DG_i)} \cdot T \cdot 8760 \right] \cdot \kappa_i \cdot \quad (9)$$

$$Cost_{EL} = \frac{CC(DG_i) \cdot CRC \cdot (1 - TR_{Paid} \cdot RVP)}{8760 \cdot CPF(DG_i) \cdot (1 - TRP)} + \frac{Cost_{FOM}(DG_i)}{8760 \cdot CPF(DG_i)} + 10^3 * Cost_{VOM}(DG_i) + 10^6 * Fuel_{Price}(DG_i) \cdot Heat_{Rate}(DG_i) \cdot \quad (10)$$

S.t:

$$CRC = \frac{D_{Rate} \cdot (1 + D_{Rate})}{(1 + D_{Rate})^{LT_{DER}} - 1} \cdot \quad (11)$$

The power production of each DER is calculated using the (12).

$$SPL(MSub_i) = \frac{RAF(DG_i) \cdot \sum_{j=1}^{NLP_i} P_j}{ALDF(DG_i)} .. \quad (12)$$

The RAF coefficient represents the coefficient of capacity of the DER to the mean power of delivery [22], which is defined by the randomness of the wind and solar resources, so as to be able to predict the randomness of wind and solar production in calculating the resource capacity. This coefficient can be obtained based on the available data on the intensity of the sun's radiation and wind speed.

2.4. Medium voltage feeder modeling

After analyzing the initial population and choosing distribution resources and distribution substations, and then removing the candidate distribution substations that were not selected, and removing the candidate feeders connected to those substations, we examine where the obtained graph connected or not connected [23]. Then, the optimal routing of the feeders is done by the Minimum Spanning Tree Algorithm of the feeders and the costs are calculated [24].

The costs of MV feeders are calculated according to formula (13):

$$MF_{FC=} Cons_{FC}^{MF} + Loss_{FC}^{MF} + Out_{FC}^{MF} \cdot \quad (13)$$

The cost of construction is equal to:

$$Cons_{FC}^{MF} = \sum_{i=1}^{N_{SMF}} CC(MF_i) \cdot \varepsilon_{df} \cdot L_i \cdot \quad (14)$$

The cost of energy losses is calculated according to the following formula:

$$Loss_{FC}^{MF} = \sum_{i=1}^{N_{SMF}} \left[I^2(MF_i) \cdot R_i \cdot \varepsilon_{df} \cdot L_i \cdot \frac{\rho \cdot T \cdot 8760}{1000} \right] . \quad (15)$$

Moreover, the cost of subscriber power outage will be equal to:

$$Out_{FC}^{MF} = \sum_{i=1}^{N_{SMF}} \left\{ \varepsilon_{df} \cdot L_i \cdot DD(MF_i) + DR(MF_i) \cdot \left[\sum_{j=1}^{N_{LMSub,i}} \sum_{k=1}^{NLP_i} P_k - \sum_{j=1}^{N_{LDER,i}} \frac{P(DG_i)}{RAF(DG_i)} \right] \cdot OCR \cdot T \cdot 8760 \right\} \quad (16)$$

The flow of MV feeders is obtained from the load distribution calculations according to the following constraints:

$$I(MF_i) < I_{max}(MF_i), \qquad \forall i \in S_{SMF} \cdot \quad (17)$$

$$\sum_{j=1}^{N_{UMF,i}} VD\left(MF_j\right) < VD_{MV,max}, \quad \forall i \in \{S_{MSub} | \lambda_i = 1\} \cdot \quad (18)$$

S.t:

$$VD\left(MF_j\right) = \left(R_j \cdot PF_j + X_j \cdot \sqrt{1 - PF_j^2} \right) \cdot \varepsilon_{df} \cdot L_j \cdot \frac{I\left(MF_j\right)}{1000 \cdot V_{MV}} \cdot 100 \cdot \quad (19)$$

2.5. HV substation modeling

The cost of HV substation includes the cost of construction, the cost of losses and the cost of subscriber's power outage as follows from (20) [18]:

$$HSub_{FC} = Cons_{FC}^{HSub} + Loss_{FC}^{HSub} + Out_{FC}^{HSub} \cdot \quad (20)$$

The construction cost of the Sub-distribution substation is equal to:

$$Cons_{FC}^{HSub} = CC(HSub) \cdot S(HSub) \cdot \gamma_i \cdot \quad (21)$$

S represents the size of the Sub-distribution substation, which is calculated by calculating the connecting load value according to (22) and processing the calculated number in one of the standard sizes of 3, 8, 15, 25, 30 or 50 MVA; it will be obtained.

$$SPL(HSub) = \sum_{m=1}^{N_{LMSub,i}} \left[\frac{\sum_{j=1}^{NLP_m} P_j}{ALDF(MSub_m)} - \sum_{m=1}^{N_{LDG,i}} \frac{P(DG_m)}{RAF(DG_m)} \right]. \quad (22)$$

The cost of energy losses of the Sub-distribution substation is calculated according to (23):

$$Loss_{FC}^{HSub} = [P_{NLL}(HSub) + P_{SCL}(HSub) \cdot TL^2(HSub) \cdot ALSF(HSub)] \cdot \rho \cdot T \cdot 8760 \cdot \gamma_i \quad (23)$$

ALSF represents the average annual loss factor, which is calculated by equation (24) [19]. TL represents the flow of Sub-distribution substation at the time of operation (in p.u.), which is calculated by equation (25):

$$ALSF(HSub) = 0.15 \cdot ALDF(HSub) + 0.85 \cdot ALDF^2(HSub) \cdot \quad (24)$$

$$TL(HSub) = \frac{\sum_{j=1}^{N_{LMSub,i}} \sum_{k=1}^{NLP_j} P_k - \sum_{j=1}^{N_{LDER,i}} \frac{P(DG_j)}{RAF(DG_j)}}{S(HSub)} \cdot \quad (25)$$

The subscriber's power outage costs of Sub-distribution substation are also calculated from formula (26):

$$Out_{FC}^{HSub} = \left[DD(HSub) + DR(HSub) \cdot \sum_{j=1}^{N_{LMSub,i}} \sum_{k=1}^{NLP_j} P_k - \sum_{j=1}^{N_{LDER,i}} \frac{P(DG_j)}{RAF(DG_j)} \right] \cdot OCR \cdot T \cdot 8760 \cdot \gamma_i \quad (26)$$

2.6. Modeling of network resiliency

Generally, in the assessment of power system resilience, the following three-step procedure is used to indicate all stages during an accident, after an accident, and during recovery. In the figure below, the overall resiliency curve is used to examine the system's resilience.

The first stage of the destruction process ($t \in [t_{pre}, t_{poe}]$): occurs between the event time t_{prr} and the end time of the incident t_{poe}. During the first stage, the level of opacity decreases and decreases from the pre-failure state of R_0 to the state after the failure of R_{pd}, and the magnitude of this decrease depends on the impact of the external factors on the system and it also depends on the length of time the accident strikes the system.

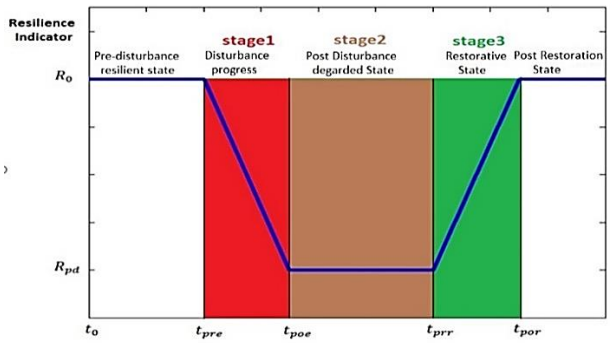

Fig. 1. The multi-phase resilience trapezoid

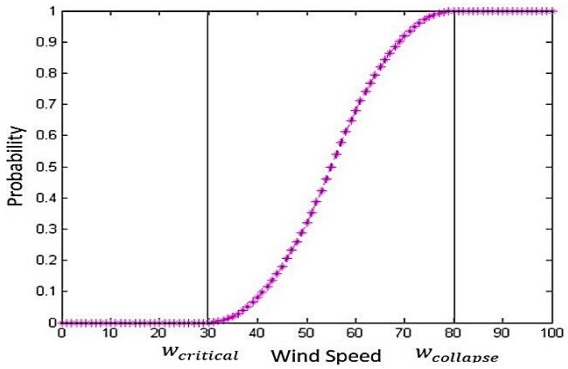

Fig. 2. Medium voltage line fragility curve

The second stage after the failure ($t \in [t_{poe}, t_{prr}]$): This step is between the end time of the incident t_{poe} and the time before the recovery t_{prr} and this time is when the system remains in a state of destruction until the team Repairs will begin after this time. In fact, the duration of this time depends on the fact that after-incident repair the third step is the recovery mode ($t \in [t_{prr}, t_{por}]$): This step starts from the start of the t_{prr} repair teams and ends when the fully retrieved system is t_{por}. In fact, this time depends on the number of repair teams, and the more repair teams are, the faster the system is retrieved.

To model the resilience of the distribution network to natural disasters, we use the concept of fragility curve that shows the probability of fragility of medium voltage lines as a function of stress conditions such as wind speed. Figure. 2 shows the curvature of the fragility of the medium-voltage distribution lines. The parameter of the critical wind speed ($w_{critical}$), which begins with the fragility of the lines and at that speed the probability of failure is zero, 30 m/s and also, the speed parameter of the falling lines ($w_{collapse}$), which probability of failure is known to be equal to one, is 80 m/s.

By combining the wind speed profiles at each stage of the simulation to this fracture curve, the probability of failure of the equipment is obtained from the time and wind speed. The relation below is the fragility function of the distribution network lines used in this paper as follows:

$$P(w_i) = \begin{cases} 0, & w \le 30 \\ 2\left(\frac{w-30}{80-30}\right)^2, & 30 \le w \le \frac{30+80}{2} \\ 1-2\left(\frac{w-80}{80-30}\right)^2, & \frac{30+80}{2} \le w \le 80 \\ 1, & w \ge 80 \end{cases} \quad (27)$$

Where $P(w_i)$ the probability of fragility of the medium voltage

lines to the function of the wind speed parameter w at the simulation teams arrived quickly and begin to recover, and this phase is over when the teams begin to work.

stage i.

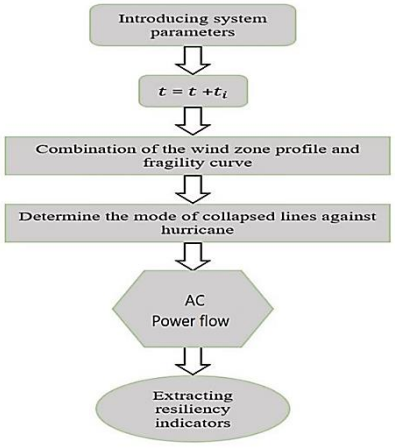

Fig. 3. Resiliency modeling processes

To model the failure of the distribution lines, we produce a uniform distributed random number, between zero and one (r ~ U (0, 1)). In this case, if at each step of the simulation $P_i(w) > r$, the medium voltage line exits from the network, and if $P_i(w) < r$, the distribution line does not exit from the network. The recovery time is considered according to the number of repair teams. After obtaining the failure states and health states of the medium-voltage lines for all the studied periods, we do load flow on the network and extract the resilient indices. In this paper, the resiliency is discussed with the hardening of medium-voltage distribution equipment and also in the presence of interconnected MGs at different speeds. Figure 3 shows the Resiliency modeling processes.

2.7. Resiliency Indicators

To evaluate the resiliency of power systems, we used some resilience indicators [17] and then we define a set of indices that show the performance of the resiliency during the various stages of the resilience trapezoid.

2.7.1 H_{fl} Index

This indicator shows how fast the resiliency is damaged and its unit is kW/hours.

$$H_{fl} = \frac{R_{pd} - R_0}{t_{poe} - t_{pre}} \tag{28}$$

2.7.2 HT_d Index

This indicator shows how much it takes from the beginning of the destruction process to the end of the destruction process and its unit is hours.

$$HT_d = t_{poe} - t_{pre} \tag{29}$$

2.7.3 H_L Index

This indicator shows how much the resiliency is damaged and its unit is kW.

$$H_L = R_0 - R_{pd} \tag{30}$$

2.7.4 t_{pd} Index

This indicator shows how much time it takes for the repair team to arrive at the scene after the damage, and it will restore the system and its unit is hours.

$$t_{pd} = t_{prr} - t_{poe} \tag{31}$$

2.7.5 H_{fr} Index

This indicator shows how fast the system is restored and its unit is kW/h.

$$H_{fr} = \frac{R_0 - R_{pd}}{t_{por} - t_{prr}} \tag{32}$$

2.7.6 HT_r Index

This indicator shows how much time it takes from the start of recovery to the network returns to normal status and its unit is hours.

$$HT_r = t_{por} - t_{prr} \tag{33}$$

2.7.7 E_{No_p} Index

This indicator shows how much energy has not been provided since the start of the destruction process until complete recovery and its unit is kW*hours.

$$E_{No\_p} = \int_{t_{pre}}^{t_{por}} R(t)\, dt \tag{34}$$

3. Test case data

The test-case is a greenfield residential area with 9 MG, 1185 load points, 1 HV substation, 342 MV candidate feeders, 55 MV candidate distribution substation and 74 candidate DG. Figure 1 shows the test-case. Figures 4,5, 6 and 7 provide more complete information about the network under study.

To investigate the resilience of the studied network, the area where studies are carried out is divided into four zones in terms of wind intensity and it is assumed that the western region is affected by wind speeds in this area, and resilient studies in this area have been carried out due to stress conditions. Figure 7 shows the wind speed of the region under study.

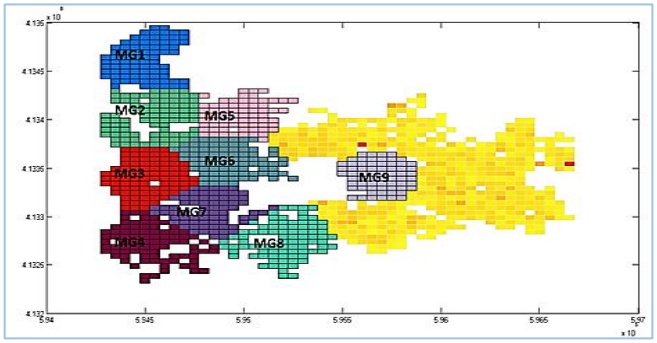

Fig. 4. Test-Case: A greenfield residential area with 9 MG

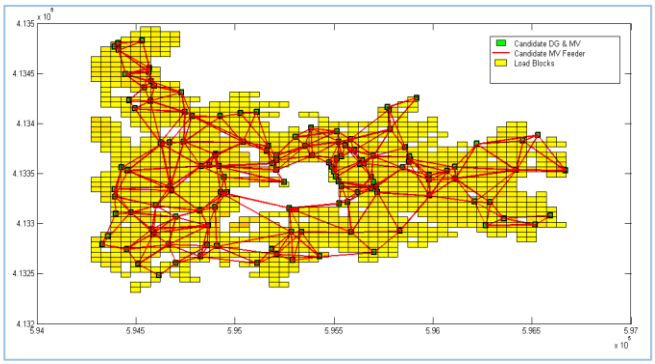

Fig. 5. The candidate routes of MV feeders on the grid.

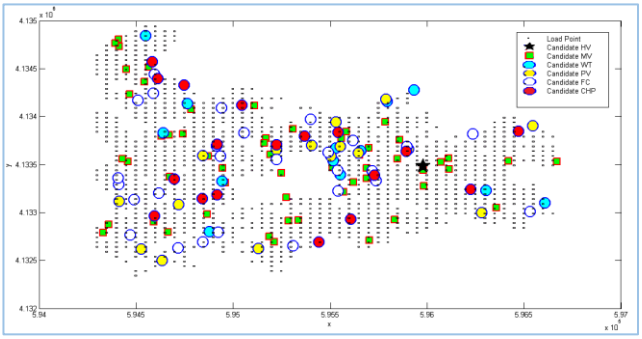

Fig. 6. Candidate points for distributing substations and HV substation as well as the type of distributed generation sources on the network.

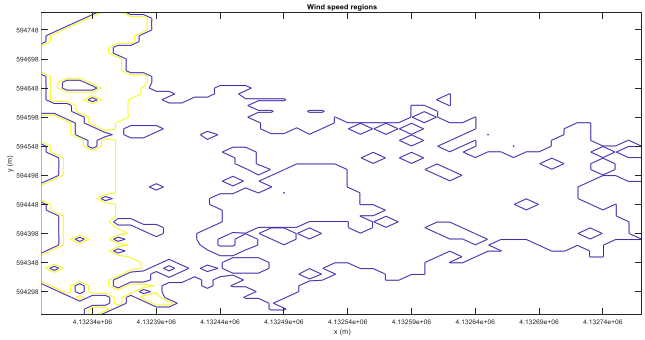

Fig. 7. Contour plot of wind speed for study area.

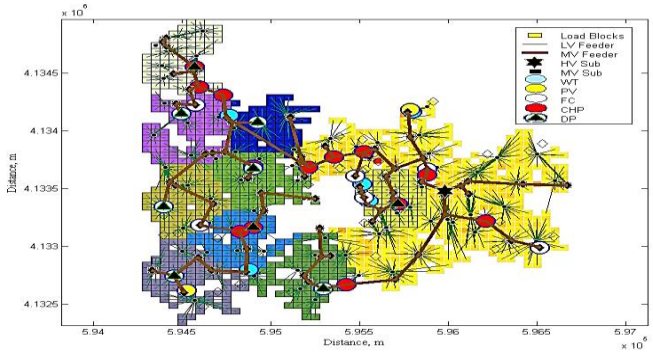

Fig. 8. Optimal configuration of planned network.

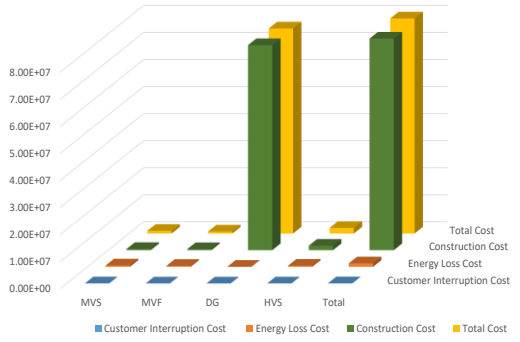

Fig. 9. Detailed costs of different parts of the network ($)

4. Results

The simulations are performed with ICA [25] optimization algorithm and the best grid arrangement is selected. In this paper, the grid arrangement and the details of the type and costs of resources selected are expressed and compared.

Table 1. Compares network costs

Network equipment	Customer Interruption Cost *($)*	Energy Loss Cost *($)*	Construction Cost *($)*	Total Cost *($)*
MVS	3.16E+04	5.12E+05	4.27E+05	9.71E+05
MVF	4.61E+01	3.57E+05	3.71E+05	7.28E+05
DG	0.00E+00	0.00E+00	7.58E+07	7.58E+07
HVS	1.25E+04	4.01E+05	1.64E+06	2.05E+06
TOTAL	4.42E+04	1.27E+06	7.82E+07	7.95E+07

Table 2. Comparison of network costs for hardening case

Construction Cost ($)	Energy Loss Cost ($)	Customer Interruption Cost ($)	Total Cost ($)	Construction Cost_R ($)	Total Cost_R ($)
3.70E+05	3.57E+05	4.61E+01	7.27E+07	3.88E+05	7.45E+05

Table 3. Input data to simulate resilience process

Storm start time (h)	Storm end time (h)	storm duration (h)	Repair start time after the storm (h)	Number of repair teams	Repair time (For each feeder) (h)
3	7	4	3	1	1

Figure 8 shows the optimal network arrangement that shows the location of the distribution substations, HV substation (HVS), the type of distributed generation sources, the feeder path, as well as the load points fed by each post, as shown in Fig 8. At least one controllable resource is selected on each micro-grid. Figure 9 shows the costs of different parts of the network, along with details.

To increase network resiliency, medium voltage feeders have been hardening, which has led to an increase in the costs of MV feeders. The following table compares the cost of MV feeders in normal and reinforced case. As seen in table 2, the hardening of medium voltage feeders increases network costs, but improved network resilience.

The study area is divided into four different zones with different wind speed and assumed that the westernmost region was affected by. The storm is assumed to begin at 3 hours and continue until 7 hours. During this period, the storm results fail of a part of the medium voltage lines. The repare time is assume to be 3 hours after the end of storm. It is also assumed that the repair teams will fix 1 medium voltage feeder every hour and the defective feeder is recovered.

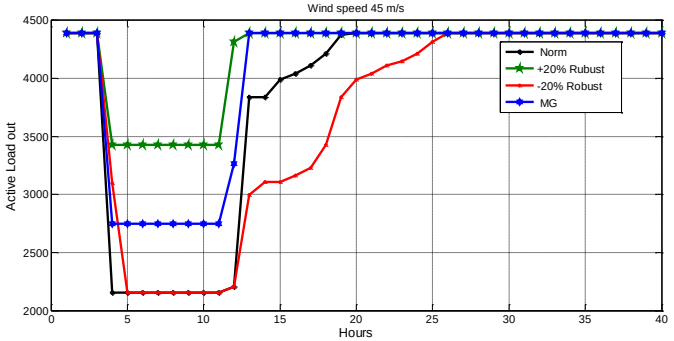

Fig. 10. Resiliency comparisons in different modes at speeds

The planned network resiliency is evaluated in four cases, 20% less, normal and 20% more hardening, and also in case of interconnected MGs. Figure 10 shows the comparison of the network

robust design in normal, reinforced and less reinforced, and interconnected MGs cases at a speed of 45 m/s. Table 2 compares different resiliency indices and shows the effectiveness of proposed solutions at speed of 45 m/s. Figure 11 shows the resilience of the network at different wind speeds. As shown in this figure, the ENS is increased with increasing of the wind speed from 45 m/s to 65 m/s. Consequently, the resiliency of the network is decreased with the increasing of the wind speed.

Table 4. Comparison of resiliency indicators at speed 45 m/s

	Norm	hardening	Less hardening	MG
H_{fl} (Kw/h)	-2200	-980	-1100	-1650
HT_d (h)	1	1	2	1
H_L (Kw/h)	2200	980	2200	1650
t_{pd} (h)	7	7	6	7
H_{fr} (Kw/h)	275	490	147	825
TH_r (h)	8	2	15	2
E_{No_p} ($K*h$)	22416.36	7377.54	28537.51	20831.67

Table 5. The total amount of power lost in different scenarios and speeds

	Wind speed (m/s)		
Type of planning	45	55	65
Less hardening	28537.51	29989.56	29989.56
Normal	22416.36	28549.89	29989.56
hardening	7377.54	21692.73	28759.97
MG	20831.67	22865.56	22865.56

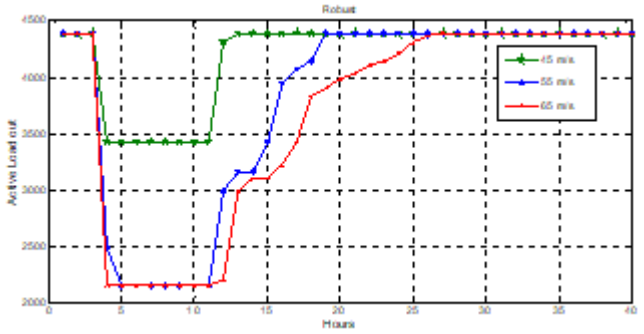

Fig. 11. Comparison of resilient network at various speeds

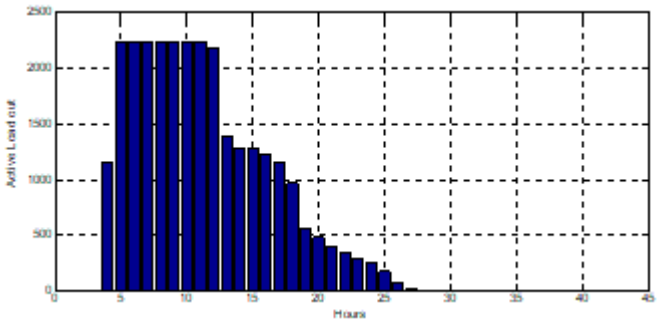

Fig. 12. The amount of ENS at wind speed 65 m/s

Figure 12 shows the effect of repairing the damaged feeders. By the recovery of defective feeders, the amount of ENS is reduced. In Table 4, the total amount of ENS is obtained for 20% less hardening mode, normal mode, 20% hardening mode and the presence of interconnected MG and for speeds of 45, 55 and 65 m/s. The table 3 shows that using one indicator alone cannot be a good criterion for assessing the resilience of distribution networks and it is necessary to use different resilience indicators together.

As can be visited in Table 5, the amount of ENS against the storm in the robust state at low wind speeds is less than the interconnected MGs mode. But at high wind speeds, the ENS in the interconnected MGs mode is less than in the robust case.

4. Conclusions

In this paper, the optimal planning of MG-based distribution networks investigated. The planning costs of network segments are compared with the reinforced MV feeders boosting network resiliency against severe hurricane. Resiliency improvement is applied to medium voltage feeders in three scenario's 20% less hardening, normal and 20% hardening against wind speeds of 45-55 65 m/s. In addition, the resiliency of advanced distribution network in the presence of microgrids is modeled, evaluated and compared with the conventional distribution networks using different resiliency metrics. Results show the effectiveness of network reinforcement against hurricane disaster conditions. According to the results the network resiliency is more increases compared to the network its associated costs. For future work, the proposed method can be implemented by defining the fragility curves of lines due to other natural disasters such as floods and earthquakes, and the results can be evaluated. Also, the resilience of the network can be evaluated in the presence of mobile energy storage devices, which are moved in critical conditions and provide the lost loads until the network is restored.

References

[1] H. Huang, K. R. Davis and H. V. Poor, **"**An Extended Model for Ecological Robustness to Capture Power System Resilience**"**, *2023 IEEE Power & Energy Society General Meeting (PESGM)*, pp. 1-5, 2023.

[2] G. F. Massari, I. Giannoccaro and G. Carbone, **"**Team Social Network Structure and Resilience: A Complex System Approach**"**, *IEEE Transactions on Engineering Management*, vol. 70, pp. 209-219, 2023.

[3] National Science and Technology Council, **"**Grand Challenges for Disaster Reduction**"**, *Subcommittee on Disaster Reduction*, 2005.

[4] S. Bahramara, R. Khezri and M. H. Haque, **"**Resiliency-Oriented Economic Sizing of Battery for a Residential Community: Cloud Versus Distributed Energy Storage Systems**"**, *IEEE Transactions on Industry Applications*, vol. 60, pp. 1963-1974, 2024.

[5] D. Carramiñana, A. M. Bernardos, J. A. Besada and J. R. Casar, **"**Enhancing Health Care Infrastructure Resiliency Through an Agent-Based Simulation Methodology**"**, *2023 International Conference on Information and Communication Technologies for Disaster Management (ICT-DM)*, pp. 1-4, 2023.

[6] K. Khanna and M. Govindarasu, **"**Resiliency-Driven Cyber–Physical Risk Assessment and Investment Planning for Power Substations**"**, *IEEE Transactions on Control Systems Technology*, vol. 32, pp. 1743-1754, 2024.

[7] Tushar, Z. Nie, A. Srivastava and S. Basumallik, **"**Measuring and Enabling Transmission Systems Resiliency With Renewable Wind Energy Systems**"**, *IEEE Transactions on Industry Applications*, vol. 60, pp. 2321-2331, 2024.

[8] A. Tavakoli, M. E. Haque, S. Saha, M. T. Arif, N. Mendis and A. M. T. Oo, **"**Power Management and Control of a Hybrid Islanded Power System to Ensure Resiliency and Economic Operation**"**,

2018 IEEE Industry Applications Society Annual Meeting (IAS), pp. 1-7, 2018.

[9] M. Panteli, D. N. Trakas, P. Mancarella and N. D. Hatziargyriou, "Boosting the Power Grid Resilience to Extreme Weather Events Using Defensive Islanding", IEEE Transactions on Smart Grid, vol. 7, pp. 2913-2922, 2016.

[10] M. Panteli, C. Pickering, S. Wilkinson, R. Dawson and P. Mancarella, "Power System Resilience to Extreme Weather: Fragility Modeling, Probabilistic Impact Assessment, and Adaptation Measures", IEEE Transactions on Power Systems, vol. 32, pp. 3747-3757, 2017.

[11] A. Arab, A. Khodaei , S. K. Khator, K. Ding, A. Emesih and Z. Han , "Stochastic Pre-hurricane Restoration Planning for Electric Power Systems Infrastructure", IEEE Transactions on Smart Grid, vol. 6 , pp. 1046 - 1054 . 2015.

[12] Xu. Wang, Z. Li, M. Shahidehpour, and C. Jiang, "Robust Line Hardening Strategies for Improving the Resilience of Distribution Systems With Variable Renewable Resources", IEEE Transactions on Sustainable Energy, Vo. 10, pp. 386 – 395, 2019.

[13] S. Ma, S. Li, Z. Wang and F. Qiu, "Resilience-Oriented Design of Distribution Systems", IEEE Transactions on Power Systems, vol. 34, pp. 2880- 2891, 2019.

[14] S. R. Osman, B. E. Sedhom and S. S. Kaddah, "Boosting the Distribution Network Resilience via Microgrid Formation and Leveraging Emergency Demand Response Program and Tie-Lines", 2023 24th International Middle East Power System Conference (MEPCON), pp. 1-6, 2023.

[15] M. Simonov, "Dynamic Partitioning of DC Microgrid in Resilient Clusters Using Event-Driven Approach", IEEE Transactions on Smart Grid, vol. 5, pp. 2618- 2625, 2014.

[16] M. Panteli and P. Mancarella, "Operational resilience assessment of power systems under extreme weather and loading conditions", 2015 IEEE Power & Energy Society General Meeting, pp. 1-5, 2015.

[17] M. Panteli, P. Mancarella, D. N. Trakas, E. Kyriakides and N. D. Hatziargyriou, "Metrics and Quantification of Operational and Infrastructure Resilience in Power Systems", IEEE Transactions on Power Systems, vol. 32, pp. 4732-4742, 2017.

[18] R. Gholizadeh-Roshanagh, S. Najafi-Ravadanegh and S. Hosseinian, "A Framework for Optimal Coordinated Primary-Secondary Planning of Distribution Systems Considering MV Distributed Generation", IEEE Transactions on Smart Grid, vol. 9, pp. 1408-1415, 2018.

[19] M. W. Gangel and R. F. Propst, "Distribution transformer load characteristics", IEEE Trans. Power Appar. Syst, vol. 84, pp. 671–684, 1965.

[20] Y. M. Atwa, E. F. El-Saadany, M. M. A. Salama, and R. Seethapathy, "Optimal renewable resources mix for distribution system energy loss minimization", IEEE Trans. Power Syst., vol. 25, pp. 360–370, 2010.

[21] R. Gholizadeh-Roshanagh, S. Najafi-Ravadanegh and S. H. Hosseinian, "On Optimal Cost Planning of Low Voltage Direct Current Power Distribution Networks", Electric Power Components and Systems, vol. 46, pp. 1019-1028, 2018.

[22] Y. M. Atwa, E. F. El-Saadany, M. M. A. Salama, and R. Seethapathy, "Optimal renewable resources mix for distribution system energy loss minimization", IEEE Trans. Power Syst., vol. 25, pp. 360- 370, 2010.

[23] N. Biggs, "Algebraic Graph Theory", Cambridge University Press, 1974.

[24] R. C. Prim, "Shortest connection networks and some generalizations", Bell Syst. Tech. J., vol. 36, pp. 1389- 1401, 1957.

[25] E. Atashpaz-Gargari and C. Lucas, "Imperialist competitive algorithm: An algorithm for optimization inspired by imperialistic competition", IEEE Congr. Evol. Comput, pp. 4661- 4667, 2007.